Supporting Information (SI)

Adsorption of tetracycline antibiotics from aqueous solutions on nanocomposite multi-walled carbon nanotube functionalized MIL-53(Fe) as new adsorbent

Weiping Xiong[a,b], Guangming Zeng[a,b*], Zhaohui Yang[a,b*], Yaoyu Zhou[c], Chen Zhang[a,b], Min Cheng[a,b], Yang Liu[a,b], Liang Hu[a,b], Jia Wan[a,b], Chengyun Zhou[a,b], Rui Xu[a,b], Xin Li[a,b]

[a] *College of Environmental Science and Engineering, Hunan University, Changsha 410082, China;*

[b] *Key Laboratory of Environmental Biology and Pollution Control, Ministry of Education, Hunan University, Changsha 410082, China;*

[c] *College of Resources and Environment, Hunan Agricultural University, Changsha 410128, China.*

[*]Corresponding authors at: Hunan University, College of Environmental Science and Engineering, Changsha 410082, PR China. E-mail: zgming@hnu.edu.cn(G.M. Zeng); yzh@hnu.edu.cn(Z.H. Yang).

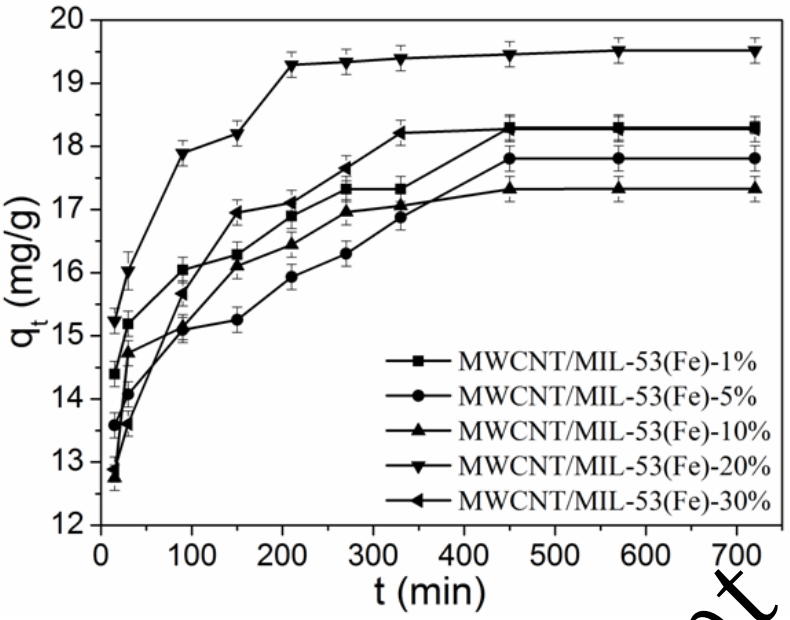

Fig. S1. The influence of different mass ratio of monomers on TCN adsorption. Experimental conditions: TCN concentration = 20 mg·L^{-1}; adsorbent loading = 1 g·L^{-1}; temperature = 25 °C; initial pH = 7. Error bars represent the standard deviation of triplicate samples.

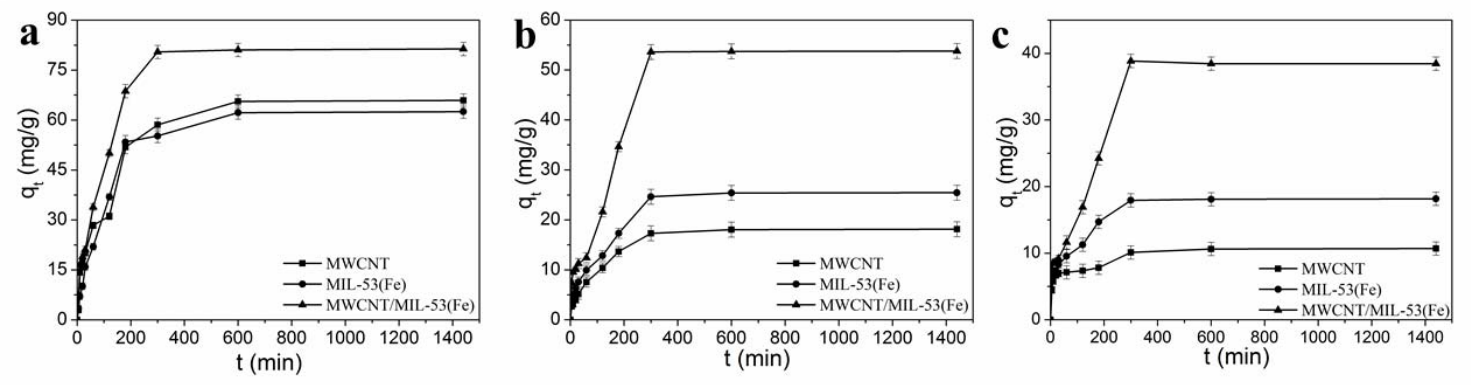

Fig. S2. The effect of time on TCN (a), OTC (b) and CTC (c) adsorption. Reaction conditions: TCN, OTC and CTC concentration = 20 $mg \cdot L^{-1}$, respectively; adsorbent loading = 0.2 $g \cdot L^{-1}$; temperature = 25 °C; initial pH = 7. Error bars represent the standard deviation of triplicate samples.

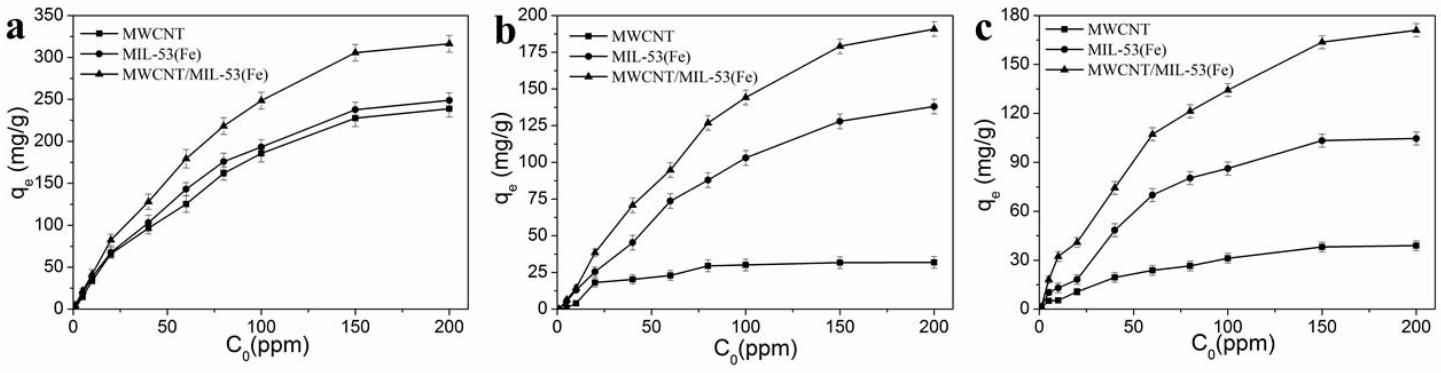

Fig. S3. The effect of pollutant concentration on TCN (a), OTC (b) and CTC (c) adsorption. Reaction conditions: adsorbent loading = 0.2 $g \cdot L^{-1}$; temperature = 25 °C; initial pH = 7. Error bars represent the standard deviation of triplicate samples.

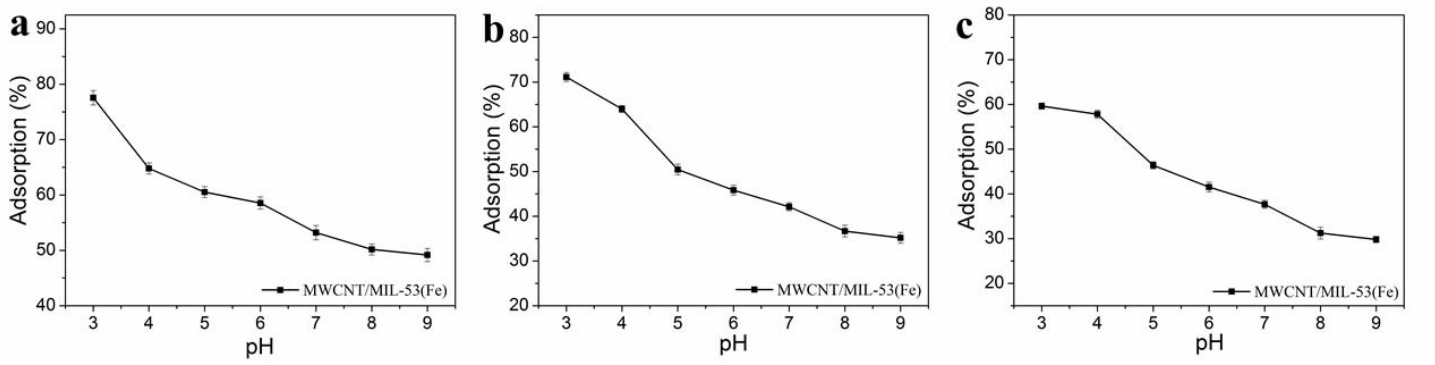

Fig. S4. Effects of solution pH of MWCNT/MIL-53(Fe) on adsorption of TCN(a), OTC(b) and CTC(c). Reaction conditions: TCN, OTC and CTC concentration = 20 $mg \cdot L^{-1}$, respectively; adsorbent loading = 0.2 $g \cdot L^{-1}$; temperature = 25 °C. Error bars represent the standard deviation of triplicate samples.

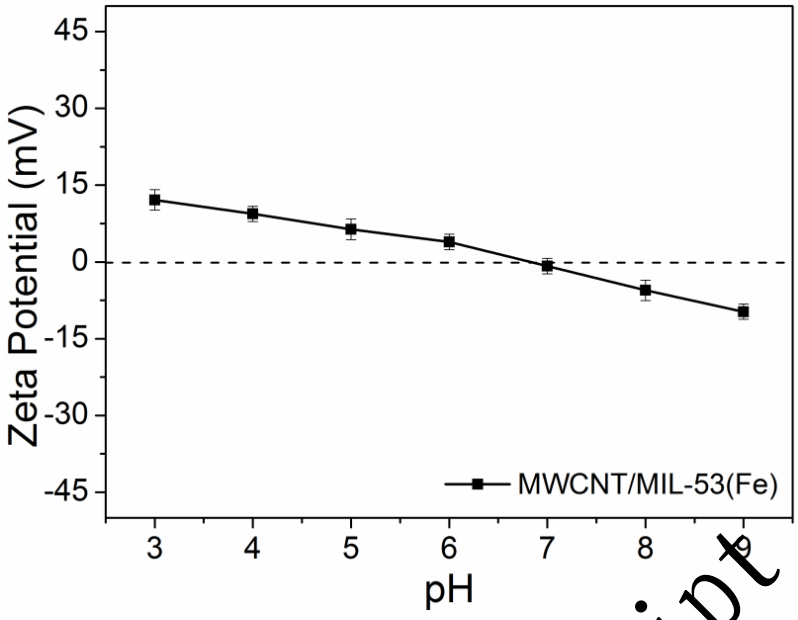

33 Fig. S5. The zeta potential of MWCNT/MIL-53(Fe) at varying pH. Error bars

34 represent the standard deviation of triplicate samples.

35

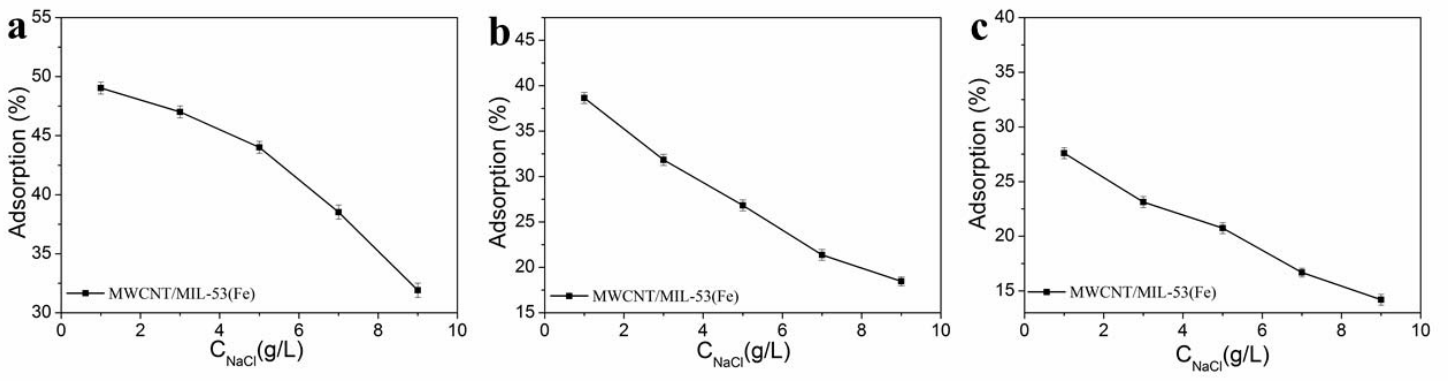

Fig. S6. Effects of ionic strength of MWCNT/MIL-53(Fe) on adsorption of TCN (a), OTC (b) and CTC (c). Error bars represent the standard deviation of triplicate samples. Reaction conditions: TCN, OTC and CTC concentration = 20 mg·L^{-1}, respectively; adsorbent loading = 0.2 g·L^{-1}; temperature = 25 °C; initial pH = 7. Error bars represent the standard deviation of triplicate samples.

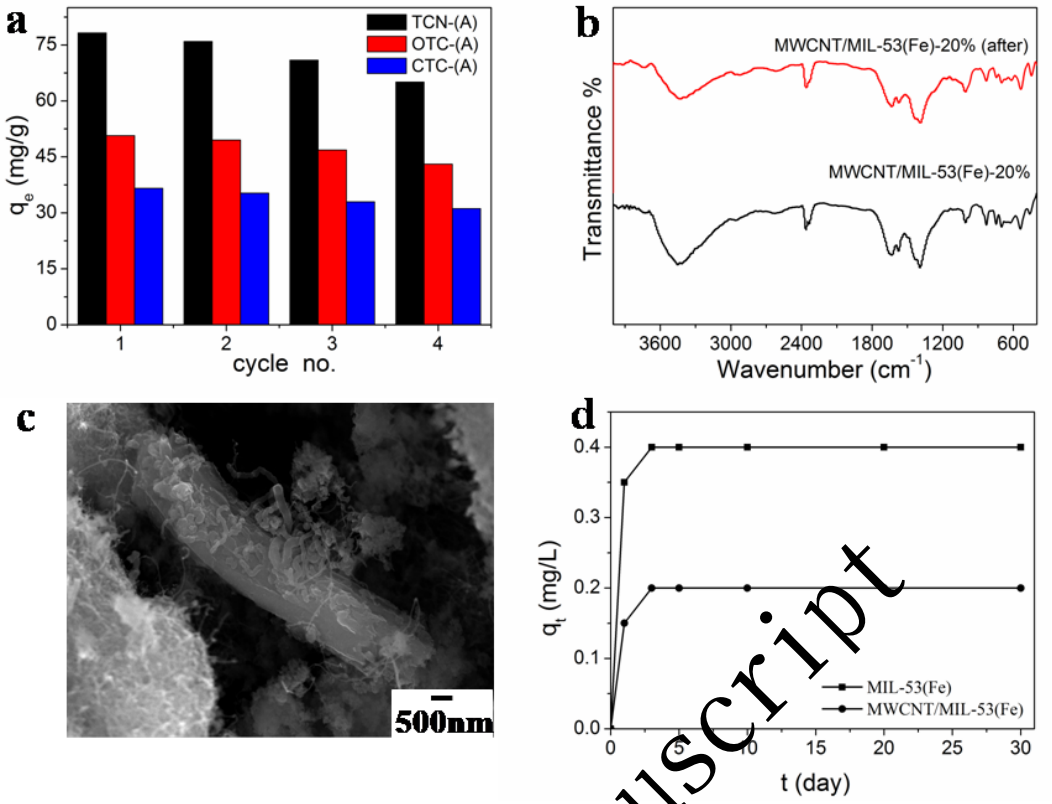

Fig. S7. (a) Recyclability of adsorbents for four adsorption runs, (C_0 = 20 mg·L^{-1}, A is MWCNT/MIL-53(Fe); (b) FT-IR spectra and (c) SEM of the adsorbent after reaction for MWCNT/MIL-53(Fe); (d) the concentration of iron ions precipitated from the adsorbent.

47 **Table S-1** The maximal adsorption capacity of TCS on different adsorbents.

Adsorption materials	contaminant	q_m (mg/g)	Isotherm model	References
MWCNT/MIL-53(Fe)	TCN	364.37	Langmuir	Present Study
	OTC	325.59		
	CTC	180.68		
Stevensite	TCN	127.1	Freundlich	R. Antón-Herrero et al.(2017)
	OTC	126.1		
	CTC	139.9		
soil 1(pH 4.5, clay 41 %)/ soil 2(pH 4.4, clay 33 %)	TCN	29.6/ 15.9	Pseudo-first-order	D. Fernández-Calviño et al.(2015)
	OTC	28.3/ 11.1		
	CTC	26.1/ 13.4		
graphene oxide	TCN	313.48	Freundlich	Gao et al.(2012)
	OTC	212.31		
alkali-acid modified magnetic biochar	TCN	286.91	Freundlich	Tang et al.(2018)
Magnetic crosslinked resins	TCN	105.34	Langmuir	Zhang et al.(2014)
Rice husk biochar	TCN	86.21	Pseudo-second-order	Jing et al.(2014)
Granular activated carbon	TCN	85.29	Langmuir	Liu et al.(2017)
MIL-101(HCl)/ MIL-101(HF)	OTC	115.34/ 91.58	Freundlich	Hu et al.(2016)
$ZnFe_2O_4$/CNTs	OTC	140.9	Langmuir	Lu et al.(2016)
Zn-[2-methylimidazolate] frameworks	OTC	28.3	Pseudo-second-order Langmuir	S.F.d.S.J. Dos et al.(2015)
hybrid silicate	OTC	207.47	Langmuir	Tian et al.(2016)
WO650	CTC	30.00	Langmuir	Ding et al.(2012)
Fe-N,N-SBA15	CTC	33.11	Langmuir	Zhang et al.(2015)
Rectorite	CTC	177.70	Langmuir	Lv et al.(2012)

Graphene oxide functionalized magnetic particles	CTC	42.6	Langmuir	Lin et al. (2013)

References

Antón-Herrero, R., García-Delgado, C., Alonso-Izquierdo, M., García-Rodríguez, G., Cuevas, J., Eymar, E., 2017. Comparative adsorption of tetracyclines on biochars and stevensite: Looking for the most effective adsorbent, Appl. Clay. Sci. https://doi.org/10.1016/j.clay.2017.12.023.

Da Silva, J. D. S. F., Malo, D. L., Bataglion, G. A., Eberlin, M. N., Ronconi, C. M., Júnior, S. A., de Sá, G. F., 2015. Adsorption in a fixed-bed column and stability of the antibiotic oxytetracycline supported on Zn (II)-[2-Methylimidazolate] frameworks in aqueous media, Plos one. 10, e0128436.

Ding, R., Zhang, P.F., Seredych, M., Bandosz, T.J., 2012. Removal of antibiotics from water using sewage sludge- and waste oil sludge-derived adsorbents, Water. Res. 46, 4081-4090.

Fernández-Calviño, D., Bermúdez-Couso, A., Arias-Estévez, M., Nóvoa-Muñoz, J. C., Fernández-Sanjurjo, M. J., Álvarez-Rodríguez, E., Núñez-Delgado, A., 2015. Kinetics of tetracycline, oxytetracycline, and chlortetracycline adsorption and desorption on two acid soils, Environ. Sci. Pollut. R. 22, 425-433.

Gao, Y., Li, Y., Zhang, L., Huang, H., Hu, J., Shah, S. M., Su, X., 2012. Adsorption and removal of tetracycline antibiotics from aqueous solution by graphene oxide, J. Colloid. Interf. Sci. 368, 540-546.

68 Hu, T., Lv, H., Shan, S., Jia, Q., Su, H., Tian, N., He, S., 2016. Porous structured
69 MIL-101 synthesized with different mineralizers for adsorptive removal of
70 oxytetracycline from aqueous solution, Rsc. Adv. 6, 73741-73747.
71 Jing, X.R., Wang, Y.Y., Liu, W.J., Wang, Y.K., Jiang, H., 2014. Enhanced adsorption
72 performance of tetracycline in aqueous solutions by methanol-modified biochar,
73 Chem. Eng. J. 248, 168-174.
74 Liu, P., Wang, Q., Zheng, C., He, C., 2017. Sorption of sulfadiazine, norfloxacin,
75 metronidazole, and tetracycline by granular activated carbon: kinetics,
76 mechanisms, and isotherms, Water. Air. Soil. Poll. 228, 129.
77 Lin, Y., Xu, S., Li, J., 2013. Fast and highly efficient tetracyclines removal from
78 environmental waters by graphene oxide functionalized magnetic particles.
79 Chem. Eng. J. 225, 679e685.
80 Lu, C., Guan, W., Qin, F., Gou, H., Luo, Y., 2016. One-pot approach to synthesize
81 ZnFe2O4/ CNTs magnetic composites for the fast removal of oxytetracycline
82 hydrochloride from aqueous solutions, Fresen. Environ. Bull. 25, 3363-3371.
83 Lv, G.C., Wu, L.M., Wang, X.L., Liao, L.B., Wang, X.Y., 2012. Adsorption of
84 chlortetracycline from water by rectories, Chin. J. Chem. Eng. 20, 1003-1007.
85 Tang, L., Yu, J.F., Pang, Y., Zeng, G.M., Deng, Y.C., Wang, J.J., Ren, X.Y., Ye, S.J.,
86 Peng, B., Feng, H.P., 2018. Sustainable efficient adsorbent: Alkali-acid modified
87 magnetic biochar derived from sewage sludge for aqueous organic contaminant
88 removal, Chem. Eng. J. 336, 160-169.

89 Tian, G., Wang, W., Zong, L., Kang, Y., Wang, A., 2016. A functionalized hybrid
90 silicate adsorbent derived from naturally abundant low-grade palygorskite clay
91 for highly efficient removal of hazardous antibiotics, Chem. Eng. J. 293,
92 376-385.
93 Zhang, M., Li, A., Zhou, Q., Shuang, C., Zhou, W., Wang, M., 2014. Effect of pore
94 size distribution on tetracycline adsorption using magnetic hypercrosslinked
95 resins, Micropor. Mesopor. Mat. 184, 105-111.
96 Zhang, Z.Y., Lan, H.C., Liu, H.J., Qu, J.H., 2015. Removal of tetracycline antibiotics
97 from aqueous solution by amino-Fe (III) functionalized SBA15, Colloids Surf. A.
98 47, 1133-138